Solar Energy Materials and Solar Cells xxx (xxxx) xxx–xxx

Contents lists available at ScienceDirect

Solar Energy Materials and Solar Cells

journal homepage: www.elsevier.com/locate/solmat

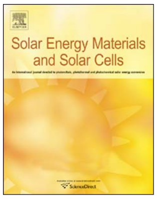

Tuning the optical and electrical properties of orthorhombic hybrid perovskite $CH_3NH_3PbI_3$ by first-principles simulations: Strain-engineering

A. Al-Shami[b,d], M. Lakhal[a,b], M. Hamedoun[a], A. El Kenz[b], A. Benyoussef[a,b,e], M. Loulidi[b], A. Ennaoui[c], O. Mounkachi[a,*]

[a] Materials and Nanomaterials Center, MAScIR Foundation, Rabat Design Center, Rue Mohamed Al Jazouli, Madinat Al Irfane, Rabat 10100, Morocco
[b] LaMCScI, Faculty of Science, Mohammed V University, B.P. 1014, Rabat, Morocco
[c] Institut de Recherche en Energie Solaire et Energies Nouvelles (IRESEN), Morocco
[d] Department of Physics, Faculty of Science, Sana'a University, Sana'a, Yemen
[e] Hassan II Academy of Science and Technology, Rabat, Morocco

ARTICLE INFO

Keywords:
First principles calculation
Strain
Orthorhombic hybrid perovskite
$CH_3NH_3PbI_3$
Photovoltaic
Solar cells

ABSTRACT

Perovskite based solar cells such as orthorhombic hybrid perovskite $CH_3NH_3PbI_3$ (OHP- $CH_3NH_3PbI_3$) have shown extraordinary power conversion efficiencies exceeding 20%. Nevertheless, the macroscopic performances of these materials and the microscopic mechanism of the photovoltaic performance of OHP-$CH_3NH_3PbI_3$ based solar cells are not fully understood yet. For example, the fluctuation and orientation of $CH_3NH_3^+$ cations and their impact on relevant processes such as charge recombination and exciton dissociation are still inadequately understood. By first-principles simulations, we show that the band gap and the transport properties of OHP-$CH_3NH_3PbI_3$ can be controlled by using simple strain conditions. With the appropriate strain, e.g. 5% (tensile or compressive), the conduction type can be rotated from an n type to a p type and vice versa, depending on the kind of process (tension or compression). This can lead to creating materials and devices with huge control over their physical properties for a wide range of applications, ranging from photovoltaic to photocatalysis.

1. Introduction

Perovskite is the most recent and promising form of research and represent a real technological breakthrough in photovoltaics (PV) technologies. Especially, the yield of perovskite-hybrid cells increased in last years, from 12% to exceed 20% [1–3]. This makes perovskite-hybrid system a promising one suited to many applications and less expensive than conventional silicon solar cells. Nowadays the best known hybrid perovskite and wish as the origin of the "breakthrough" material in the photovoltaic field is OHP-$CH_3NH_3PbI_3$. The state of the art on the crystalline, electronic and optical structures of OHP-$CH_3NH_3PbI_3$, is evolving very quickly due to the enthusiasm of researchers for this material. The spectacular success of this material is primarily due to these different properties: ambipolar transport properties, high charge carrier mobilities, diffusion lengths of carriers and the possibility of changing the optical gap by simple substitution of the halogen. Moreover, the chemical flexibility of these hybrid perovskites and their different shapes give the hope of being able to work and improve the material in the context of PV applications. The particularly feature of OHP-$CH_3NH_3PbI_3$ which distinguish it from other materials for photovoltaic applications, is the orientation of $CH_3NH_3^+$ ions that has a critical impact on the optical and electrical properties relevant for photovoltaic applications [4]. The microscopic mechanism of the high photovoltaic performance and these properties is yet to be fully understood. Among proposed microscopic pictures, one scenario is based on presence of nanoscale ferroelectric domains [5] and rearrangement of the inorganic scaffold which is intimately linked with the $CH_3NH_3^+$ ion orientation [4,6]. In this regard, it will be extremely interesting if manipulations of $CH_3NH_3^+$ ions orientation can be done. Nowadays, various approaches can be applied to engineer electronic structures, optical and electrical properties of materials and nanomaterials for PV application [7,8]. In order to use OHP- $CH_3NH_3PbI_3$ as photovoltaic materials and for other applications, it is interesting to find out a way to ameliorate their physical properties. In this study, the role of biaxial strain on OHP-$CH_3NH_3PbI_3$ and their effect on the stability, optical and transport properties was investigated. It was obvious to attempt to use strain to control those appealing anisotropies of OHP- $CH_3NH_3PbI_3$. Our results present an important advancement towards controlling physical properties of OHP- $CH_3NH_3PbI_3$ via strain engineering, with important implications to create new materials and devices for a wide range of

---

* Corresponding author.
E-mail addresses: o.mounkachi@gmail.com, o.mounkachi@mascir.com (O. Mounkachi).

http://dx.doi.org/10.1016/j.solmat.2017.06.047
Received 15 February 2017; Received in revised form 19 June 2017; Accepted 19 June 2017
0927-0248/ © 2017 Elsevier B.V. All rights reserved.

Please cite this article as: Al-Shami, A., Solar Energy Materials and Solar Cells (2017), http://dx.doi.org/10.1016/j.solmat.2017.06.047

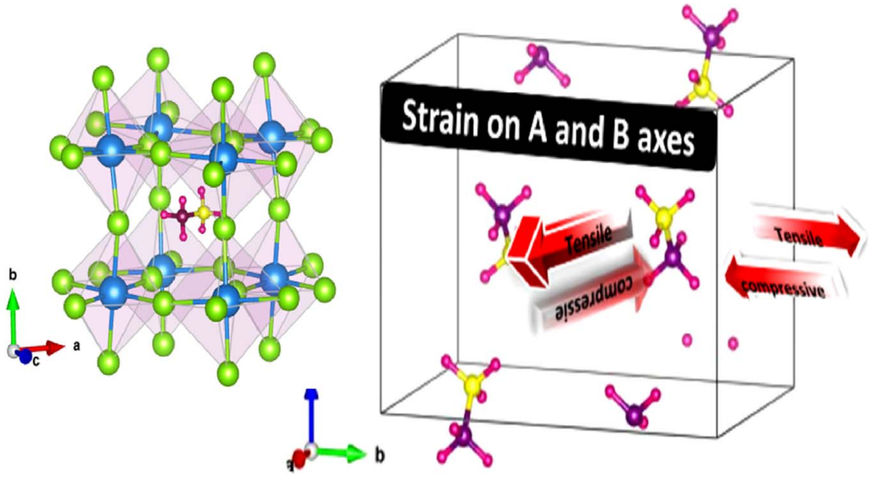

Fig. 1. OHP-$CH_3NH_3PbI_3$ unit cell and model under biaxial tensile or compressive strain (ε(xx), ε(yy) along x and y axes respectively).

Table 1
The theoretical lattice constant of OHP-$CH_3NH_3PbI_3$ in comparison with the experimental data for LDA (PZ81/LDA), GGA (PBE/GGA) and vdW (optB86b-vdW24) approximations.

	Parameter	Exp (Å) [9]	Theo (Å)	Difference
vdW	a	8.861	8.807	0.61%
	b	12.62	12.61	0.07%
	c	8.581	8.56	0.25%
GGA	a	8.861	8.548	3.53%
	b	12.62	12.32	2.38%
	c	8.581	8.475	1.24%
LDA	a	8.861	8.361	5.64%
	b	12.62	12.15	3.73%
	c	8.581	8.318	3.06%

applications. In Section 2, the details and methods to perform our calculation are given. Section 3 is devoted to the presentation and the discussion of our numerical results. In the last section, the conclusion is given.

1.1. Computational Methods

The structural and electronic properties of OHP- $CH_3NH_3PbI_3$ are investigated using the plane-wave projector-augmented wave method as implemented in the QUANTUM-ESPRESSO package. Electron–ion interactions are described using ultra soft pseudo potentials with a kinetic energy cut-off of 700 eV. Brillouin-zone integrations are performed using Monkhorst-Pack grids of special points 4 × 3 × 4 and 9 × 8 × 9 meshes for the calculations of structural and electronic properties, respectively. The OHP-$CH_3NH_3PbI_3$ primitive cell has 48 atoms, see Fig. 1a. The relaxation of lattice constants and atomic coordinates have been done using the van der Waals density functional (optB86b-vdW24) [9]. Starting from the obtained band structures the carrier mobility is calculated using deformation potential theory originally developed by Bardeen and Shockley [10] and generalized by Herring and Vogt [11]. Which is a band model including only the lattice scatterings by the acoustic deformation potential. It is based on the Boltzmann transport equation and sometimes can be simplified using the effective mass approximation. Here we use The BOLTZTRAP code [12] for the calculation of semi-classical transport coefficients through the use of Fourier expansions to solve Boltzmann equations.

Once the properties of unit cell of OHP-$CH_3NH_3PbI_3$ were obtained, the mechanical biaxial strain is imposed on the relaxed unit cell along x [100] and y[010] directions according to Eq. (1) as shown in Fig. 1b:

$$\varepsilon_{xx}(\%) = \varepsilon_{yy}(\%) = \frac{a(b) - a_0(b_0)}{(a_0(b_0))} \tag{1}$$

Where the lattice constants a(b) of OHP-$CH_3NH_3PbI_3$ unit cell are constrained to several different values, differing from the equilibrium lattice constants $a_0(b_0)$ by fractions ranging from −5% to 5% by step of 1%. The lattice constant c is obtained by allowing all atomic positions to relax to a minimum energy state under each strain. All atomic positions in each strained OHP-$CH_3NH_3PbI_3$ unit cell with constrained lattice constants ‘a′ and ‘b′ were fully optimized to obtain the lattice constant c.

2. Results and discussion

2.1. Structure and band-gap optimizations of OHP-$CH_3NH_3PbI_3$

Before determining and studying the optical and transport properties of our system, the crystalline structure of the unstrained unit cell was fully relaxed using different functional (vdW, PBE/GGA, PZ81/LDA). The initial lattice constants and atomic coordinates of OHP-$CH_3NH_3PbI_3$ structure phase were taken from experiment data [9]. The optimized lattice constants are listed in Table 1 with the available experimental values. In general, the PZ81/LDA [13] functional underestimates all the lattice constants, while the PBE/GGA [14] functional overestimates them. Our results show that the best structural descriptions are obtained using the vdW/optB86b-vdW24 functional, where the cell parameters of the relaxed structure are a = 8.807 Å, b = 12.61 Å, c = 8.56 Å. In this case the deviation with respect to the experimental data does not exceed 1% while it can reach a value up to 5.64% and 3.53% with LDA and GGA, respectively. The band gap calculations are carried out and are presented in Table 2. vdW functional gives the closest value to the experimental one and this is due to large weak vdW binding between the organic components across the inorganic framework that required to depict the structural properties of this type of organic-inorganic hybrid materials. Now that the most suitable functional to represent the properties of our system have been determined, the calculations of states density, strain and carrier mobility will be done using optB86b+ vdW24. The calculations of total density of states (TDOS) and partial density of states (PDOS) are shown in Fig. 2. In this figure, it is clear that the organic $CH_3NH_3{}^+$ cations made little contribution to the top valence and bottom conduction bands around the Fermi energy level (E_f). The main contribution to the top valence band is from the I-5p states with an overlapping of Pb-6s states. In the bottom conduction bands, the main components are Pb-6p

Table 2
The theoretical band gap of OHP-$CH_3NH_3PbI_3$ in comparison with the experimental data for LDA (PZ81/LDA), GGA (PBE/GGA) and vdW (optB86b-vdW24) approximations.

	vdW	GGA	LDA	Exp [12,13]
Band gap(eV)	1.73	1.81	1.55	1.68–1.72

Download English Version:

https://daneshyari.com/en/article/6534226

Download Persian Version:

https://daneshyari.com/article/6534226

Daneshyari.com